

NASA/CR—1998-208514

ICOMP-98-04



Effects of Tip Clearance and Casing Recess on Heat Transfer and Stage Efficiency in Axial Turbines

A.A. Ameri
AYT Corporation, Brook Park, Ohio

E. Steinthorsson
Institute for Computational Mechanics in Propulsion, Cleveland, Ohio

David L. Rigby
NYMA, Inc., Brook Park, Ohio

Prepared for the
Turbo Expo '98
sponsored by the International Gas Turbine Institute
of the American Society of Mechanical Engineers
Stockholm, Sweden, June 2-5, 1998

Prepared under Contract NAS3-27571

National Aeronautics and
Space Administration

Lewis Research Center

August 1998

Acknowledgments

This work was sponsored by the Smart Green Engine Project managed at NASA Lewis Research Center by Mr. Kestutis Civinskas. The authors wish to express their gratitude to Dr. Raymond Gaugler, chief of the Turbine Branch, Mr. Ned Hannum chief of the Turbomachinery and Propulsion Systems Division as well as to Dr. Louis Povinelli chief scientist of the Turbomachinery and Propulsion Systems Division of NASA Lewis Research Center and Director of ICOMP for their support and encouragement of this work. As always we had the benefit of helpful suggestions offered by Mr. Robert Boyle of NASA Lewis Research Center. Some of the computations were performed on the CRAY-C90 of NAS at NASA Ames Research Center.

Trade names or manufacturers' names are used in this report for identification only. This usage does not constitute an official endorsement, either expressed or implied, by the National Aeronautics and Space Administration.

Available from

NASA Center for Aerospace Information
7121 Standard Drive
Hanover, MD 21076
Price Code: A03

National Technical Information Service
5287 Port Royal Road
Springfield, VA 22100
Price Code: A03

EFFECTS OF TIP CLEARANCE AND CASING RECESS ON HEAT TRANSFER AND STAGE EFFICIENCY IN AXIAL TURBINES

A. A. Ameri

AYT Corporation, Brook Park, Ohio, USA

E. Steinhorsson

Institute for Computational Mechanics in Propulsion (ICOMP)

NASA Lewis Research Center, Cleveland, Ohio, USA

David L. Rigby

NYMA, Inc. NASA Lewis Group, Cleveland, Ohio, USA

ABSTRACT

Calculations were performed to assess the effect of the tip leakage flow on the rate of heat transfer to blade, blade tip and casing. The effect on exit angle and efficiency was also examined. Passage geometries with and without casing recess were considered. The geometry and the flow conditions of the GE-E³ first stage turbine, which represents a modern gas turbine blade were used for the analysis. Clearance heights of 0%, 1%, 1.5% and 3% of the passage height were considered. For the two largest clearance heights considered, different recess depths were studied. There was an increase in the thermal load on all the heat transfer surfaces considered due to enlargement of the clearance gap. Introduction of recessed casing resulted in a drop in the rate of heat transfer on the pressure side but the picture on the suction side was found to be more complex for the smaller tip clearance height considered. For the larger tip clearance height the effect of casing recess was an orderly reduction in the suction side heat transfer as the casing recess height was increased. There was a marked reduction of heat load and peak values on the blade tip upon introduction of casing recess, however only a small reduction was observed on the casing itself. It was reconfirmed that there is a linear relationship between the efficiency and the tip gap height. It was also observed that the recess casing has a small effect on the efficiency but can have a moderating effect on the flow underturning at smaller tip clearances.

NOMENCLATURE

| | |
|----------------------|--|
| <i>A</i> | inlet area |
| <i>C</i> | axial chord |
| <i>C_p</i> | constant pressure specific heat |
| <i>d</i> | distance upstream of the leading edge expressed as a percent of the axial chord. |
| <i>G</i> | clearance height, expressed as percent of the annulus |

| | |
|----------------------|---|
| <i>h</i> | height (see Fig. 1) |
| <i>k</i> | heat transfer coefficient- wall heat flux/(T ₀ -T _w) |
| <i>k</i> | thermal conductivity or kinetic energy of turbulence/RT ₀ |
| <i>N</i> | rotation rate |
| <i>Pr</i> | Prandtl number= (μC _p)/k |
| <i>R</i> | recess depth (see Fig. 1) or gas constant for air |
| <i>Re</i> | Reynolds number |
| <i>T</i> | temperature/T ₀ |
| <i>Tu</i> | turbulence intensity $(\sqrt{\frac{2k}{3}})/V$ |
| <i>V</i> | total velocity/ $\sqrt{RT_0}$ |
| <i>v*</i> | friction velocity, $(\sqrt{\tau_w})/\rho$ |
| <i>X</i> | distance measured from the leading edge (see Fig.1) |
| <i>y</i> | normal distance from wall |
| <i>y⁺</i> | dimensionless distance from a wall, $y^+ = y \frac{v^*}{\nu}$ |
| <i>m</i> | mass flow rate |
| <i>γ</i> | specific heat ratio |
| <i>μ</i> | viscosity |
| <i>τ_w</i> | wall shear stress |
| <i>ρ</i> | density |
| <i>ω</i> | $(2\pi NC)/(\sqrt{RT_0})$ |

Subscripts

| | |
|----------|-------------------------|
| <i>t</i> | total conditions |
| <i>w</i> | wall |
| <i>0</i> | total inlet condition |
| <i>1</i> | base case (see Fig. 14) |

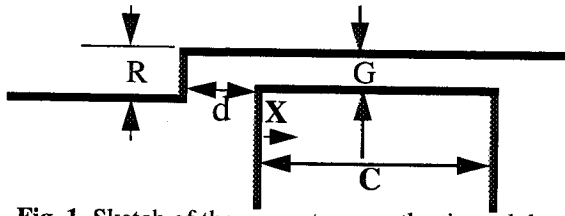


Fig. 1 Sketch of the geometry near the tip and the nomenclature

TABLE 1. Summary of cases

| G | d | R/G |
|-----|-----|-----------------------|
| 0 | --- | 0. (no casing recess) |
| 1. | --- | 0.(no casing recess) |
| 1.5 | --- | 0.(no casing recess) |
| 1.5 | 15% | 0.5, 1. (level), 1.5 |
| 1.5 | 25% | 0.5, 1. (level), 1.5 |
| 3 | --- | 0.(no casing recess) |
| 3 | 25% | 1/3, 2/3, 1. (level) |

INTRODUCTION

The tip clearance is responsible for a significant portion of losses in turbines. Much attention is being paid to reduction in losses due to the tip clearance flows since other sources of loss are not as amenable to manipulation as the tip clearance losses. Blade tips are also susceptible to burnouts and oxidation due to the large thermal loading on and near the blade tips. Losses and heat load in the tip region increase as the tip gap widens. This increase in losses and the increased heat load is particularly deleterious to the operation of engines under certain periods of operation, such as during take off when the clearance gap is wider. The tip clearance also widens as the engine gets older.

Tip and casing treatments are used to improve the efficiency and reduce the tip heat transfer. Among the various treatments used for the blade tip are the use of squealer type blades, the most widely used among them being the double squealer tip which is simply a recess in the blade tip. Ameri et al. (1997) simulated the flow and heat transfer due to tip recess and showed that the effect on efficiency was insignificant and also the heat transfer issues were not ameliorated by the tip recess. An experimental study performed by Kaiser and Bindon (1997) showed that for their 1 1/2 stage turbine, the recessed tip had a negative effect on the efficiency. Neither the numerical conclusions of Ameri et. al nor those of Kaiser and Bindon were in agreement with the popular belief that the tip recess increases the efficiency by reducing the tip clearance flow.

Another method employed to reduce the tip clearance losses is the use of the casing recess. In this work in addition to the examination of the effect of the clearance height we examine the effect of casing recess on the tip and casing heat transfer and its influence on efficiency. There is some experimental work available in the open literature, namely that of Haas and Kofsky (1979), which addresses the effect of the casing recess on the efficiency for a small turbine. Their experiments show that the maximum efficiency is achieved using a casing recess at level with the tip of the blade. There is also one numerical study

(Briley et al. 1991) of turbine blade flow that does include tip clearance and casing recess, however their effects are not separated.

The task of calculation of the heat transfer and particularly efficiency in terms of absolute magnitudes is a formidable one especially for complex flow passages such as the flow passage at hand. A comparative study is however possible if special care is taken to retain as much similarity between the grid distribution for the cases considered as possible.

In the section to follow we will give a brief description of the numerical method used in the simulations. Next the flow field near the tip and the recess will be discussed and salient features pointed out. Then we will present the heat transfer results which include the blade surface near the tip, the tip and casing heat transfer. Next we will present the results of the calculations of the exit angle. Finally we will present the results of the calculations of efficiency for a range of gap heights and casing recesses and close by presenting a summary and the conclusions.

COMPUTATIONAL METHOD

The simulations in this study were performed using a multi-block computer code called TRAF3D.MB (Steinhorsson et al. 1993). This code is a general purpose flow solver designed for simulations of flows in complicated geometries. The TRAF3D.MB code solves the full compressible Reynolds averaged, Navier-Stokes equations using a multi-stage Runge-Kutta based multigrid method. It uses the finite volume method to discretize the equations. The code uses central differencing together with artificial dissipation to discretize the convective terms. The overall accuracy of the code is second order. The present version of the code (Rigby et al. 1996, 1997a and Ameri et al. 1997) employs the $k-\omega$ turbulence model developed by Wilcox (1994a, 1994b) with subsequent modifications by Menter (1993). The model integrates to the walls and no wall functions are used. For heat transfer a constant value of 0.9 for turbulent Prandtl number, Pr_t is used. A constant value for $Pr=0.72$ is used. Viscosity is a function of temperature through a 0.7 power law (Schlichting, 1979) and C_p is taken to be a constant.

GEOMETRY AND THE GRID

Figure 1 shows a sketch of the problem and the definitions of some of the variables used in the study. As tabulated in Table 1, four gap clearances of $G=0\%$, 1%, 1.5% and 3% of the passage height are used. The 0% and 1% cases are run without casing recess. For the two wider gaps, the recess heights are varied. For the 1.5% gap case there are two sets of calculations for d , namely $d=15\%$ and 25% of the chord. For the 3% gap $d=25\%$ of the chord is used.

The blade chosen for this study is a generic modern gas turbine rotor blade, the General Electric E³ (Energy Efficient Engine) design which is detailed in two NASA reports (Halila et al., 1982 and Timko, 1982). The rotor blades have a constant axial chord length of 2.87 cm. and an aspect ratio of 1.39. Figure 2(a) shows the blade geometry and the basic features of the grid, The insets (b) and (c) show the details of the grid on the tip and on the casing showing the recess geometry. The grid is generated using a commercially available computer program called GridProTM. The grid topology is quite complex and the grid for a geometry with tip

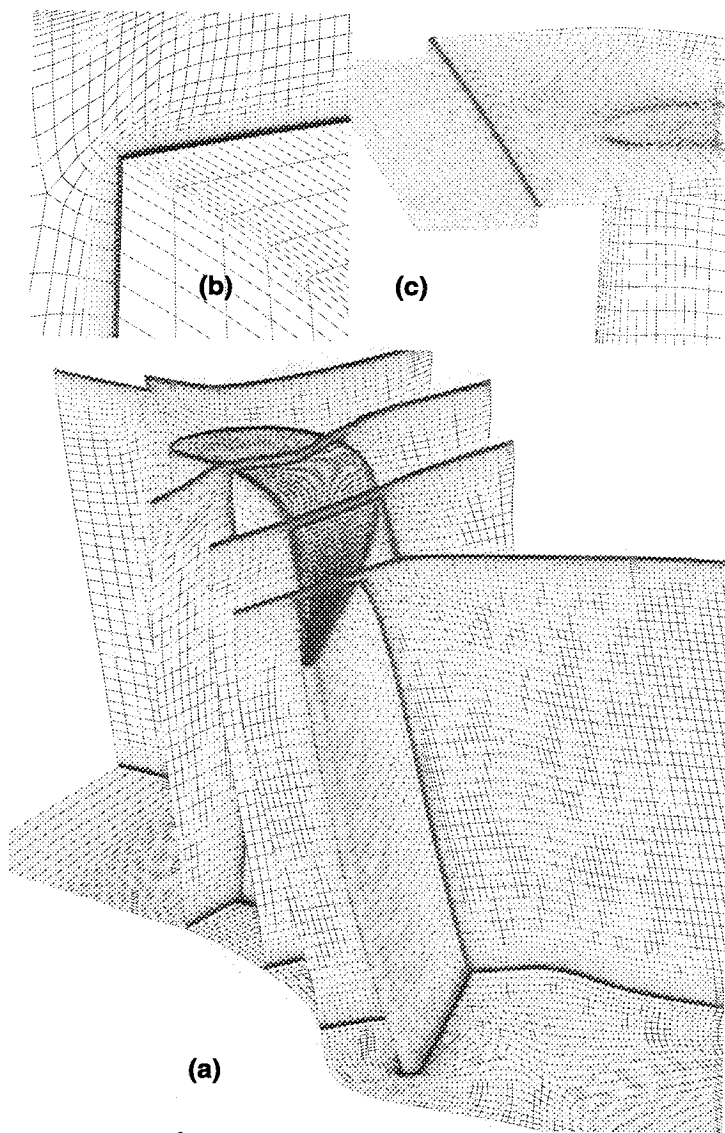


Fig. 2 GE, E³ first stage rotor blade. (a) Overall grid. (b) details of the tip grid near the edge and (c) details of the casing grid

clearance and casing recess consists of 310 blocks. Once the grid is generated, for reasons of computational efficiency, the blocks are merged to produce fewer number of blocks namely 29 blocks for runs with casing recess and 26 blocks for runs without casing recess. This was done using the Method of Weakest Descent as described in Rigby et al. (1997b) and Rigby (1996). In order to keep the grids for the many cases considered in this work as similar as possible we have assured that the general topology is the same for all the cases considered. Therefore after the first grid was generated, the grids for the remaining similar cases could be generated rather quickly. The viscous grid is generated by embedding grid lines where needed. We have required that the stretching ratio not to exceed 1.25 for the viscous grid away from the no-slip surfaces. The distance to the first cell center adjacent to solid wall is specified such that the distance in wall units, (y^+) is less than unity. This is verified and the distribution of y^+ on and

TABLE 2. Run conditions

| | |
|---|---------|
| Absolute press. ratio across the blade row | 0.44 |
| Reynolds number (based on inlet relative conditions) and blade chord. | 200,000 |
| Inlet Mach number (relative) | 0.38 |
| Dimensionless rotation rate, ω | 0.0254 |
| $T_{\text{wall}}/T_{\text{total at inlet}}$ | 0.7 |

near the tip will be given in the results section. One attractive feature of the generated grid is that as shown in Fig. 2(b) the viscous grid wraps around the blade instead of extending into the free stream. This feature of the grid improves the convergence of the solution. Near the edge of the blade, in the tip region (Fig. 2(b)) better refinement of the grid might be required for more accurate results, however since we are making relative comparisons extreme measures are avoided. In spite of the above, the total number of grid points is typically around 1.3 million. 59-65 grid points are used radially within the tip clearance. 33 grid points are used to resolve the boundary layers on the blade. This does not include the “inviscid” blade to blade grid which is also quite fine. At the inlet patch the number of grid points is 85 in the pitchwise and 97 in the spanwise direction.

RUN CONDITIONS

The run conditions are provided in Table 2. The manner in which the boundary conditions are imposed both for the flow and turbulence variables are as given in Ameri et al. (1997). However for the sake of completeness the inlet boundary conditions are given in Figs. 3(a) and (b). The swirl angle in Fig. 3(a) was specified as per measurements of Timko(1982). The inlet total temperature and pressure were specified by the use of the law of the wall through the specification of the inlet boundary layer thickness at the hub and the casing. For the turbulence quantities, an inlet turbulence intensity of 8% and a length scale of 1% of axial chord was used. These values were estimated and believed to be representative of the conditions existing at the inlet of the blade row.

RESULTS AND DISCUSSION

General Remarks

All the cases presented herein have been converged to better than 0.01% mass flow error. The residual for all the cases dropped 6 to 7 orders of magnitude. The heat transfer and efficiency results have been checked for convergence by comparing solutions after consecutive runs of 300 iterations. The present calculations match the experimental mass flow rate to within 0.5% percent. As described earlier, in order to achieve accurate resolution of heat transfer on surfaces, the grid was generated to result in dimensionless distance of the first cell center off the walls to be below unity. Figure 4 shows a typical distribution of dimensionless wall distance on and near the tip. It can be seen that the goal has been met.

Clearance gaps chosen for the study of recessed casing are relatively wide since tip clearance effects are stronger for larger

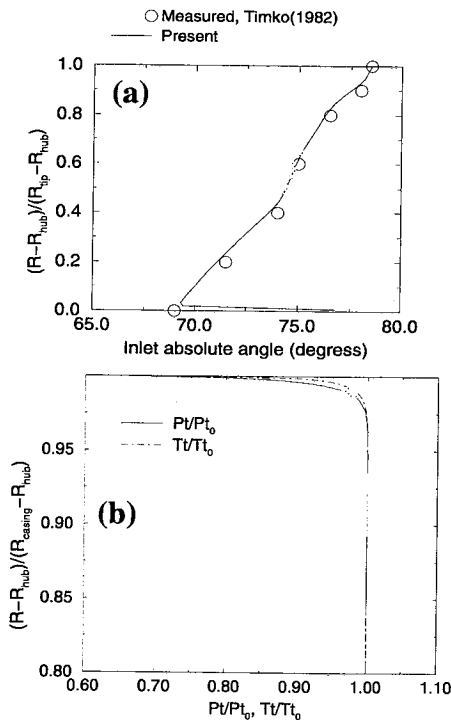


Fig. 3 (a) Inlet absolute swirl angle and (b) inlet total temperature and total pressure

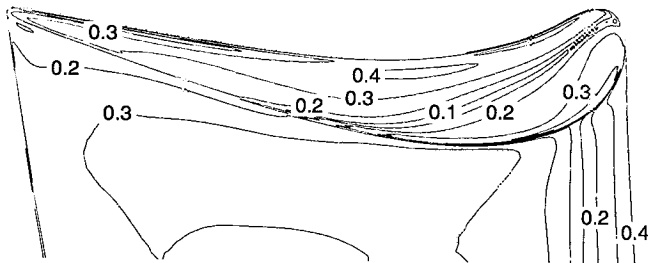


Fig. 4 Distribution of y^+ on and near the blade tip. $G=3\%$

gaps and the effect of recessed casing are expected to be more pronounced as was shown by Haas and Kofsky (1979).

Flow Field

Figure 5 shows streamline patterns for a 1.5% clearance gap and those for a 3% clearance gap. Both cases possess a casing recess upstream. In the two figures the edge vortex, suction side tip vortex and the larger structure which appears to be a horseshoe vortex are present. The low momentum fluid behind the recess also appears to be joining this larger structure in both of the cases. The larger tip clearance gives rise to a larger tip vortex by virtue of its larger mass flow rate through the tip. The above mentioned structures enhance the heat transfer to the blade and will be discussed further in subsequent sections. Figure 6(a) shows the region behind the casing recess. The arrows in this figure and in all subsequent ones are projections of the relative velocity vectors onto the viewing area. A distinct recirculation zone (blockage) can be discerned behind the recess. Figures 6(b)

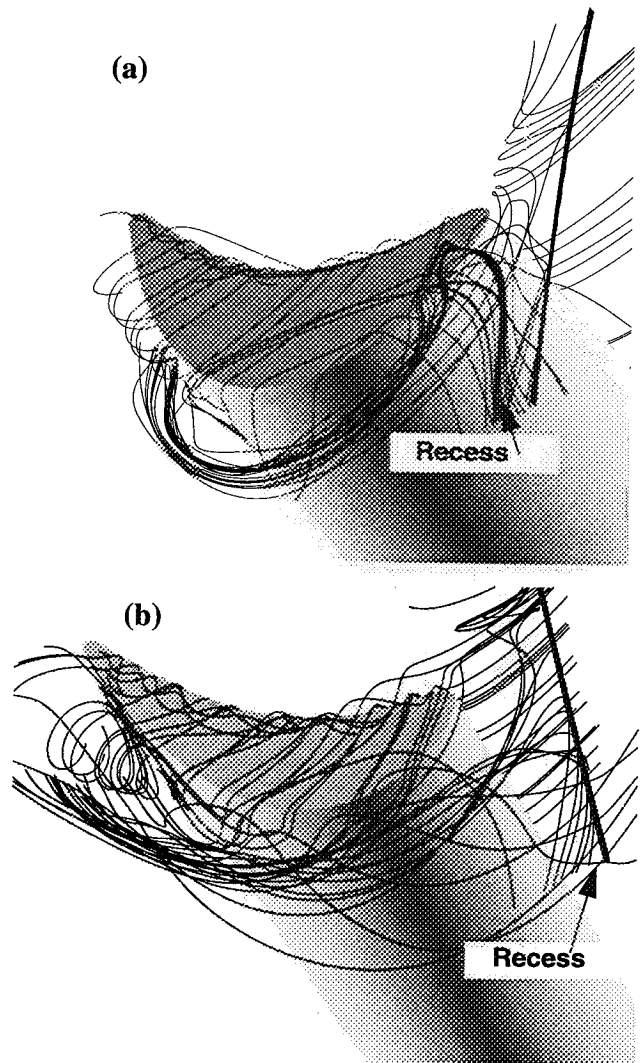


Fig. 5 (a) Streamline patterns for (a) $G=1.5\%$, $R/G=1.$ at $d=15\%$ and (b) $G=3\%$ and $R/G=1., d=25\%$

and (c) show the flow relative to the blade at a radial location mid gap of the tip clearance for the $G=1.5\%$ without and with a casing recess upstream, respectively. The modification of the flow over the tip downstream of the recess as compared to the no recess case is quite obvious from the two figures. In particular the larger secondary flow due to reduced fluid momentum behind the casing recess is quite apparent. The relative reduction in the magnitude of the velocity over the tip for the recessed case is also apparent from the two vector plots.

Further observations with the regards to the flow structure will be made in connection with heat transfer in the ensuing sections.

Heat Transfer

The present computational method has been applied to a variety of turbine heat transfer problems by using an algebraic turbulence model (Ameri and Steinthorsson 1995, 1996). The present turbulence model was tested against the heat transfer

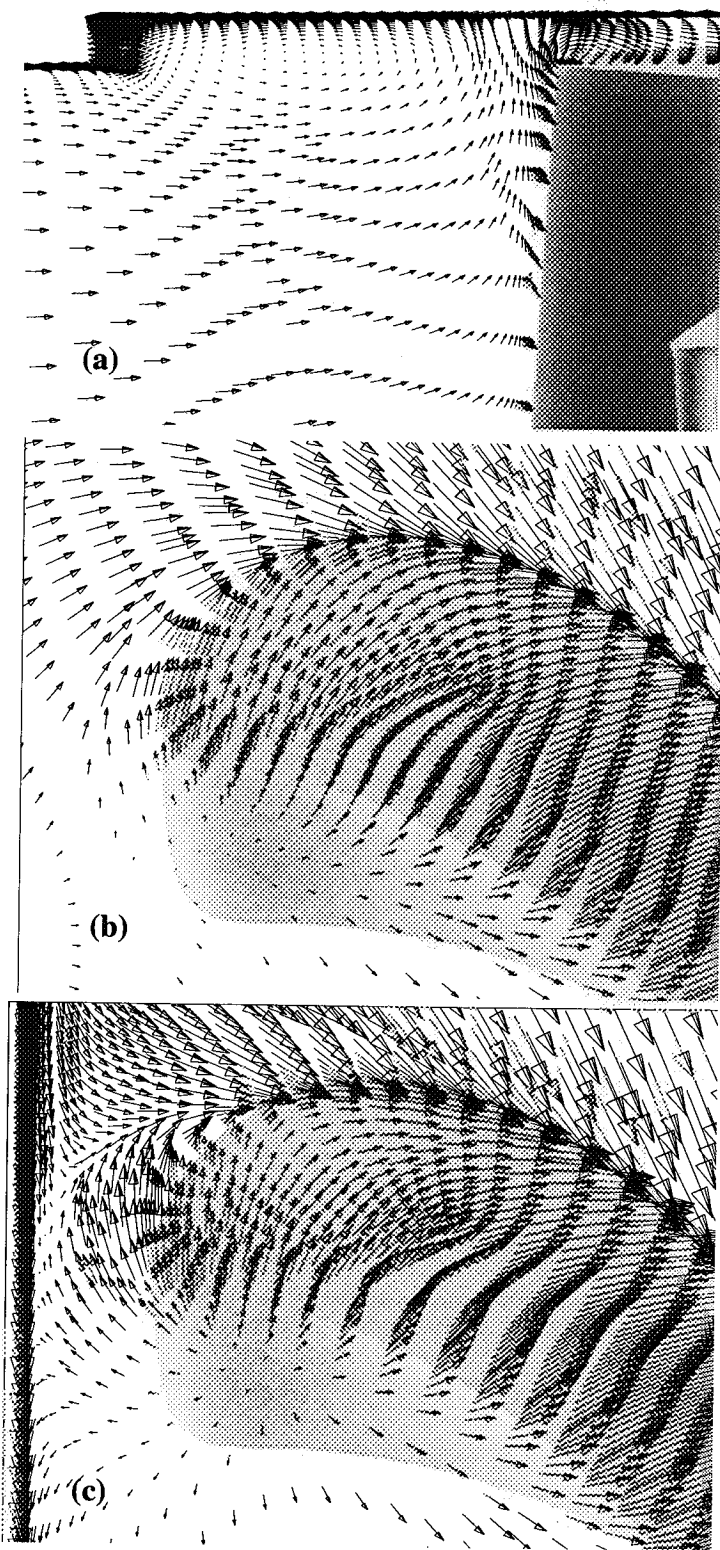


Fig.6 Velocity vectors at (a) behind the casing recess showing the recirculation zone, and radial location mid gap of the tip clearance, $G=1.5\%$ for, (b) no casing recess and (c) level recess at $d=0.15$

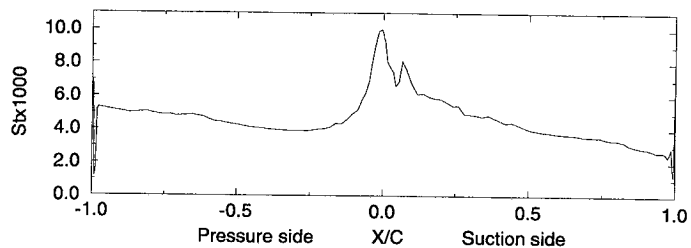


Fig. 7 Mid span blade heat transfer

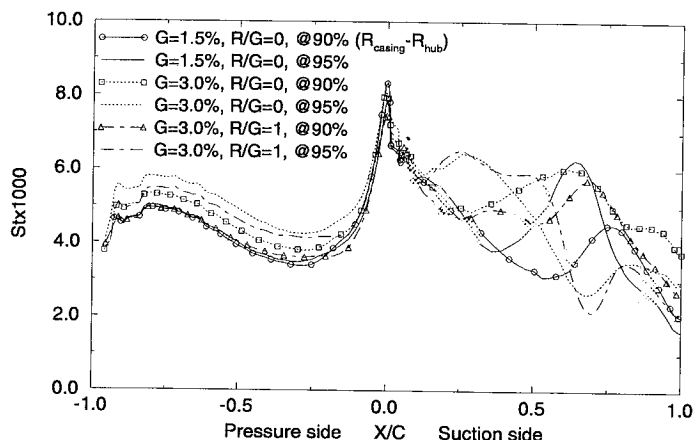


Fig. 8 Heat transfer near the tip as affected by the tip clearance height and casing recess

data of Metzger et. al. (1989) for flow over a cavity to show suitability of the model for blade tip recess flows in Ameri et al. (1997). Very good comparison using the current method for blade surface heat transfer with experimental data was achieved by Garg and Rigby (1998). Heat transfer results for internal flows can be found in Rigby et al. (1996, 1997a).

The rate of heat transfer is presented in terms of Stanton number defined as:

$$St = \frac{h}{(\dot{m}/A)_{inlet} C_p} \quad (1)$$

where h is the heat transfer coefficient based on the absolute inlet total temperature. C_p is the constant pressure specific heat (assumed a constant), \dot{m} is the mass flow rate and A is the inlet area. The ratio of \dot{m}/A is very much a constant for the cases considered.

Blade Heat Transfer. Figure 7 shows the rate of heat transfer at the mid-span. By referring to this figure and specifically the magnitude of the rate of heat transfer at the stagnation point an appreciation can be gained for the magnitude of the rate of heat transfer shown elsewhere on the blade.

Figure 8 shows the blade heat transfer rate at two locations of 90 and 95% passage height. On the pressure side, the effect of increase in tip clearance height is to increase the blade heat transfer near the tip. Also discernible is the increase in heat transfer as the tip itself is approached due to sink effect.

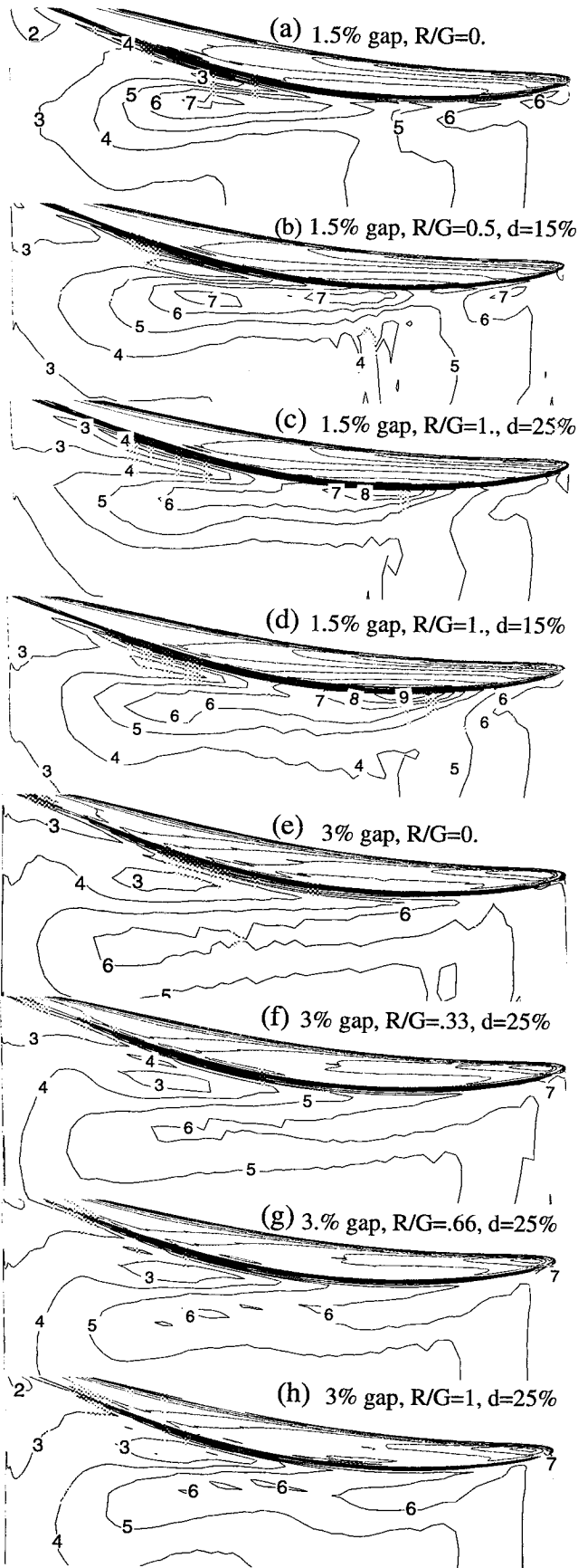


Fig. 9 Near tip suction side heat transfer. (1000x Stanton no.)

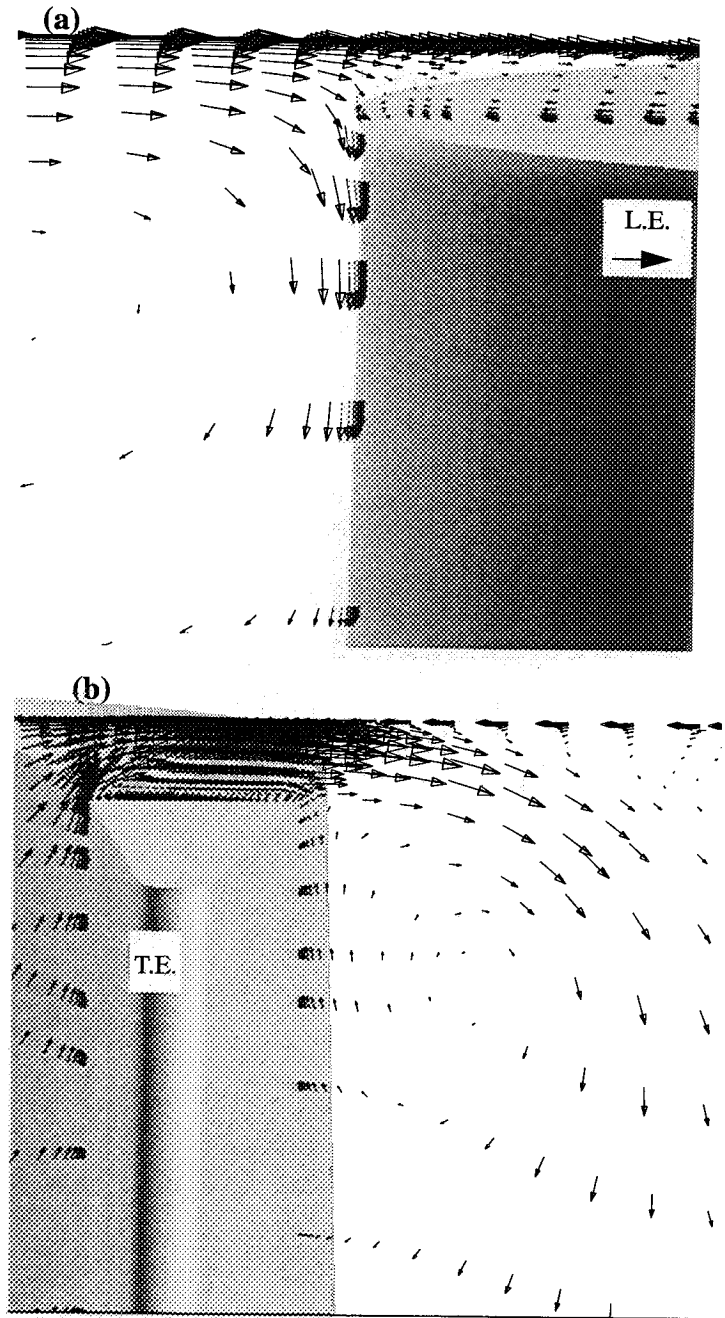


Fig. 10 Velocity vectors near the tip on the blade suction side for (a) $G=1.5\%$, $R/G=1$, and $d=15\%$ and (b) $G=3\%$, $R/G=1$.

Introduction of a casing recess causes a drop in the pressure side heat transfer.

The heat transfer on the suction side is more complex. Shown in Fig. 9 is the suction side heat transfer contours near the tip for a number of cases. The contour plots are provided for two gap clearances of 1.5% and 3% and for a range of casing recess heights as needed. Figures 9(a) and 9(e) show that the effect of doubling the gap height on the suction side heat transfer is to enlarge the area on the blade influenced by the tip vortex flow, thus raising the suction side heat transfer load. The peak heat transfer for the smaller tip clearance is larger. This could be attributed to the effect

of the secondary flow that runs across the passage toward the blade suction side. In Fig. 10(a) the velocity vectors at a location near the crown of the blade for the $G=1.5\%$, $R/G=1$, and $d=15\%$ are shown. The effect of the crossflow on the suction side of the blade is obvious from the figure. The "hot spots" near the tip in Figs. 9(b), 9(c) and 9(d) are attributable to this effect. The tip clearance flow on the other hand in Fig. 10(b) dominates the suction side of the blade. The 3% tip clearance cases all have the tip vortex dominant flows on the suction side. There is a gradual reduction of the heat loading on the suction side as the casing recess height is increased.

Tip Heat Transfer. Tip Heat transfer will be presented in the form of contour plots of Stanton number accompanied by a line plot representing the average rate of heat transfer on the blade tip as a function of axial distance.

Figure 11 shows the rate of heat transfer as measured by Stanton number on the tip of the blade for three gap clearances. The line plot shows the increasing tip clearance gap to elevate the rate of heat transfer over the upstream portion of the blade but have the opposite effect on the downstream portion. Near the trailing edge the heat transfer is mostly dominated by the size and the extent of the separation bubble.

In Fig. 12, the flow over the blade tip at three locations along the blade for the case of 3% tip clearance is presented. The separation of the flow upon entering in the gap is evident from that figure. The locations of flow reattachment in the planes considered have been marked with white arrows. The tip flow at the location farthest downstream on the blade shows that the hot gas from the core does not come in contact with the tip surface. Examination of the tip flow for smaller gaps (not shown to conserve space) revealed that the location on the tip where the flow does not reattach moves downstream as the gap narrows. Therefore the larger the gap size the larger the portion of the blade where the flow is unattached leading to smaller heat transfer rates in the downstream portion of the blade tip. Further discussion of the effect of the tip clearance height on the blade tip will be given at the end of this section.

To investigate the effect of casing recess on the tip heat transfer two gap clearances of 1.5% and 3% were considered. Figures 13(a) and (b) show the effect of casing recess upstream of the blade row for $G=1.5\%$. A range of R/G values from 0 to 1.5 was considered. The casing recess was placed at 25% chord upstream. The contour plots show the local effect of the upstream recess on the blade tip heat transfer. Looking at the peak heat transfer it can be seen that the recess on the casing reduces the peak level of heat transfer and in general the larger the recess the smaller is the peak heat transfer. The line plot at the bottom shows the integrated average of the tip heat transfer over the blade tip. The line plots show a decreasing level of tip heat transfer as a function of casing recess depth. A different set of calculations was run for the recess placed at 15% chord upstream of the blade row. Figure 14 shows the results of those runs. The line plot in Fig. 14(b) clearly shows that the effect on the tip heat transfer is larger in this case ($d=15\%$) as compared to the case of $d=25\%$ as one would expect intuitively.

Figure 15 shows the variation of the tip heat transfer as a function of recess depth for the larger 3% tip clearance. A range

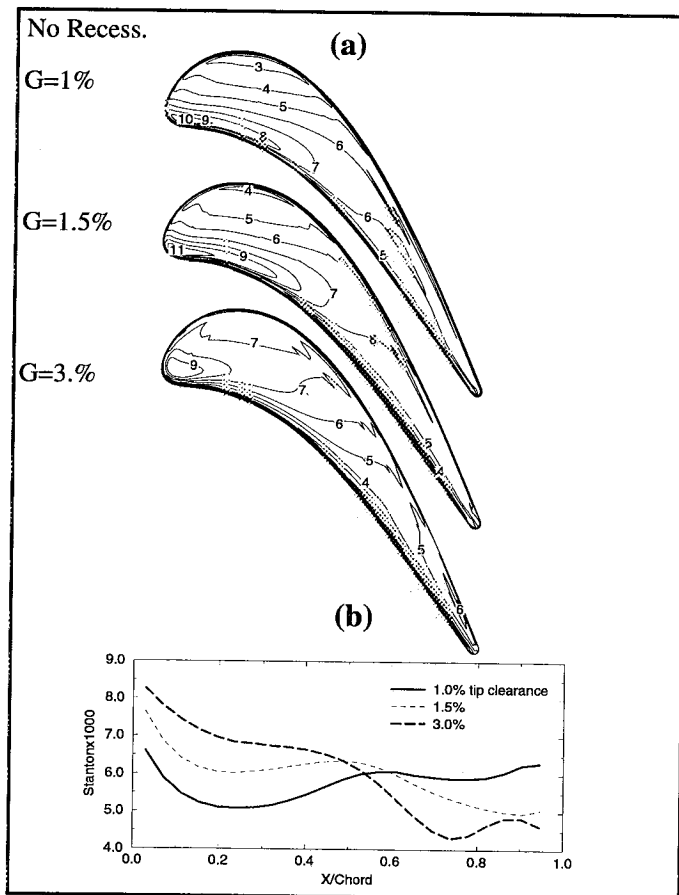


Fig. 11 (a) Contours of $1000 \times$ Stanton number over the blade tip for three gap widths and (b) line plot of the average tip heat transfer as a function of the axial distance

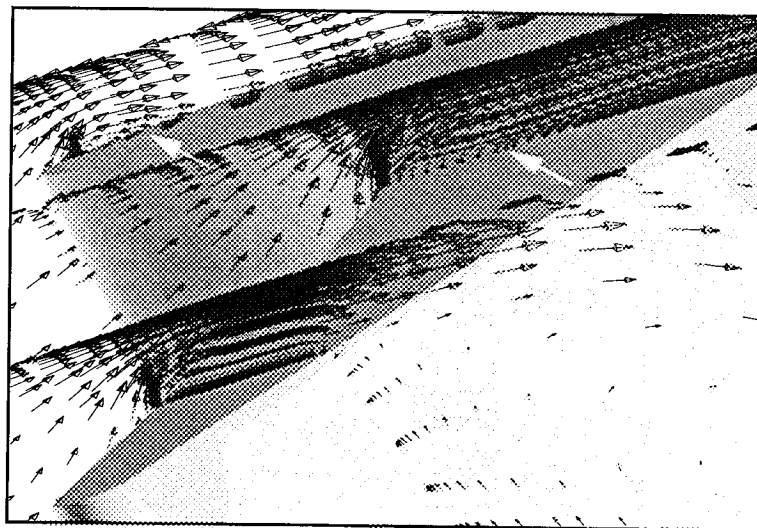
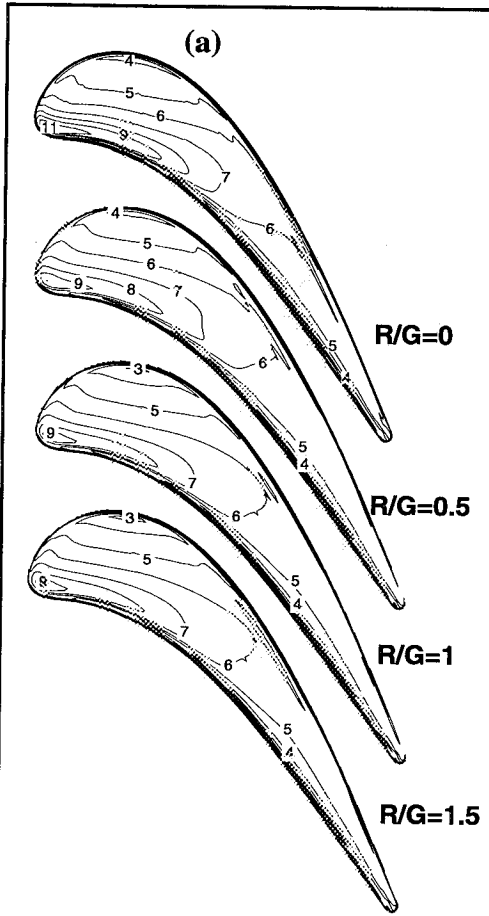


Fig. 12 Velocity vectors showing flow through the tip clearance at three locations. Observed flow reattachment is marked by the arrow.



$d=25\%$
 $G=1.5\%$

(b)

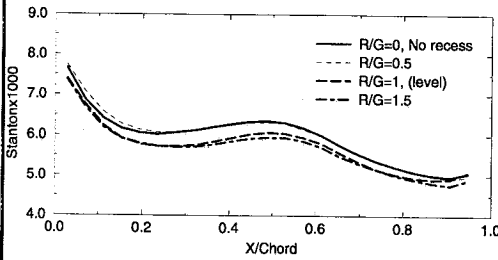
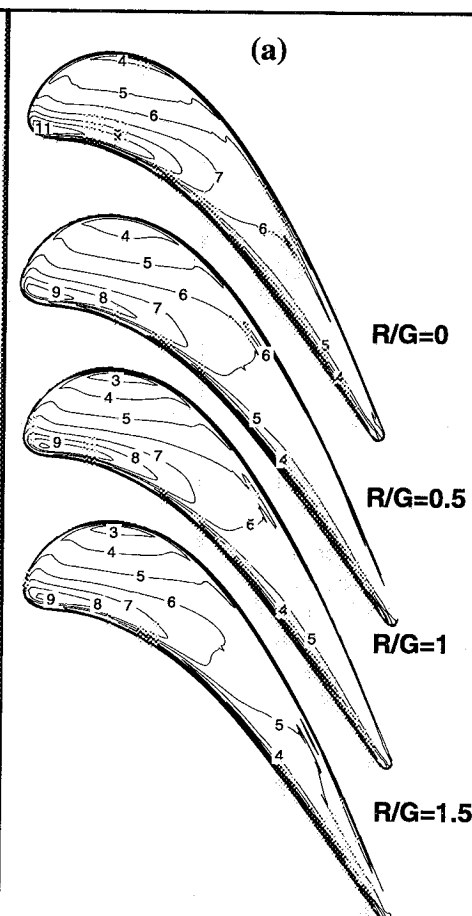


Fig. 13 (a) Contours of $1000 \times \text{Stanton}$ number over the blade tip and (b) line plots of average tip heat transfer. $d=25\%$, $G=1.5\%$



$d=15\%$
 $G=1.5\%$

(b)

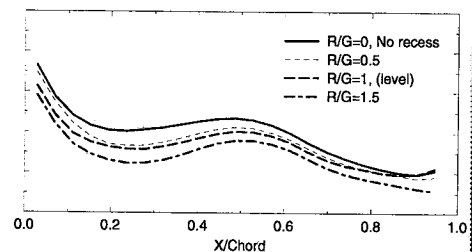
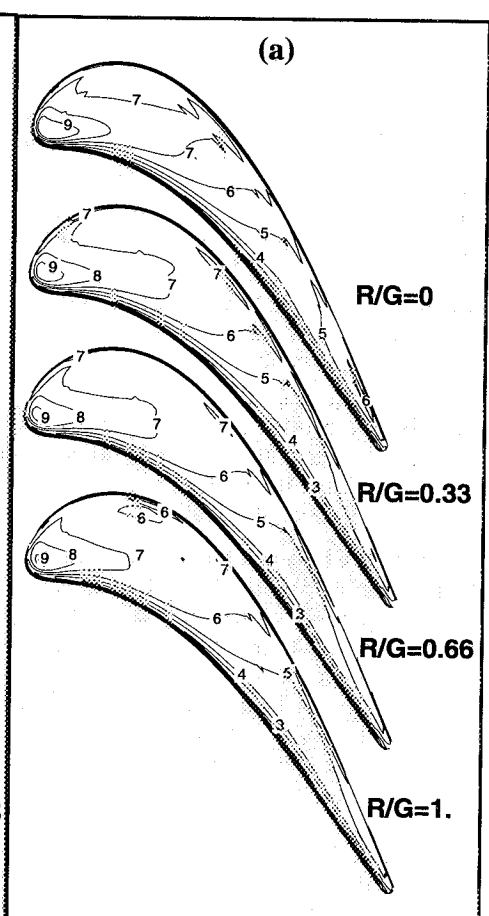


Fig. 14 (a) Contours of $1000 \times \text{Stanton}$ number over the blade tip and (b) line plots of average tip heat transfer. $d=15\%$, $G=1.5\%$



$d=25\%$
 $G=3.0\%$

(b)

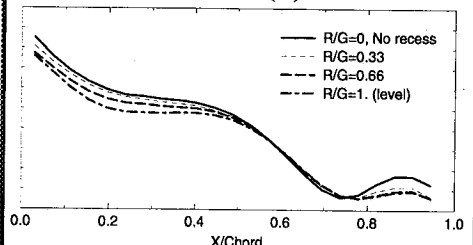
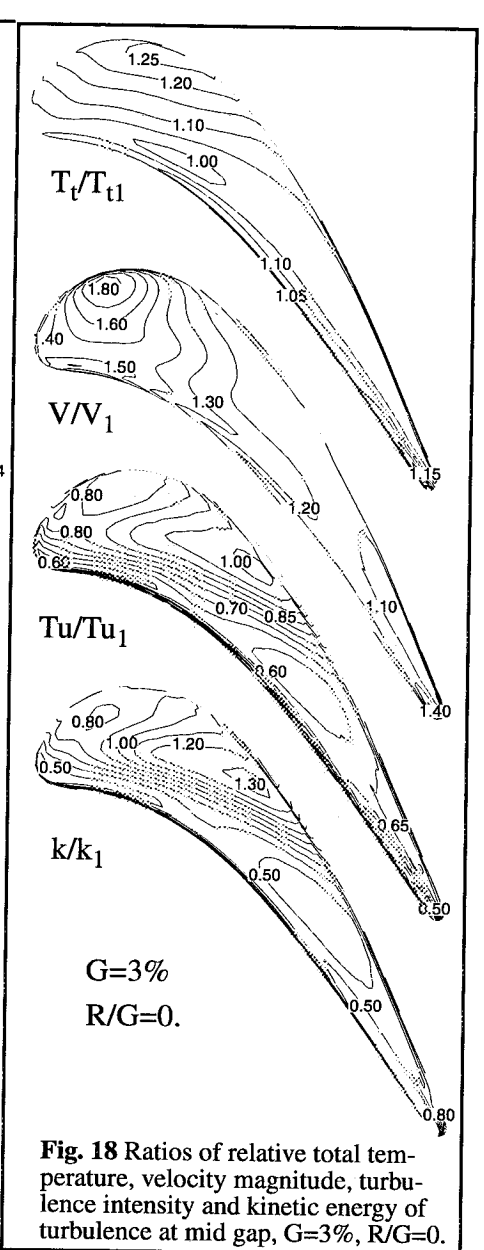
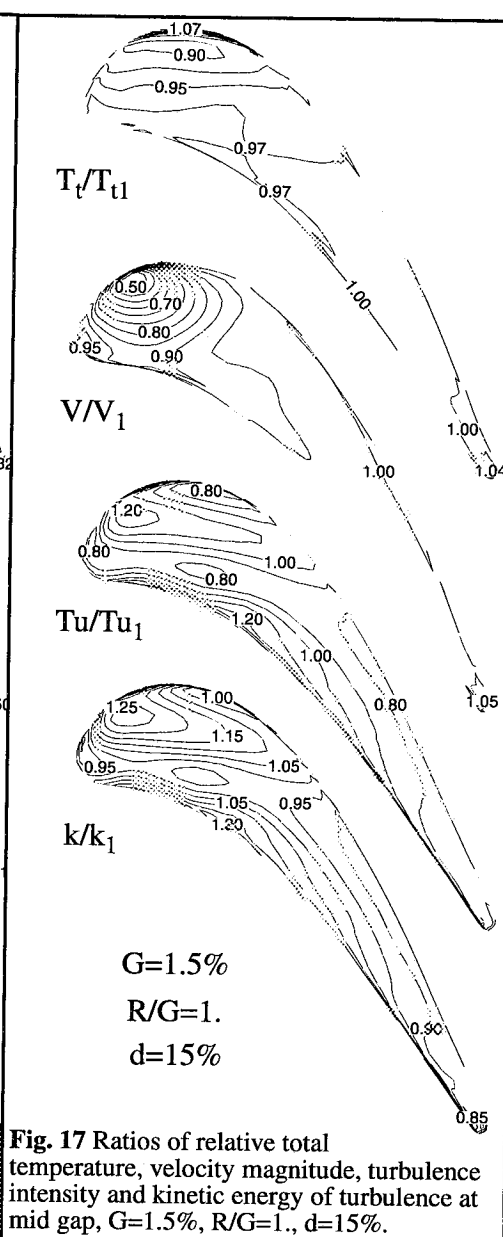
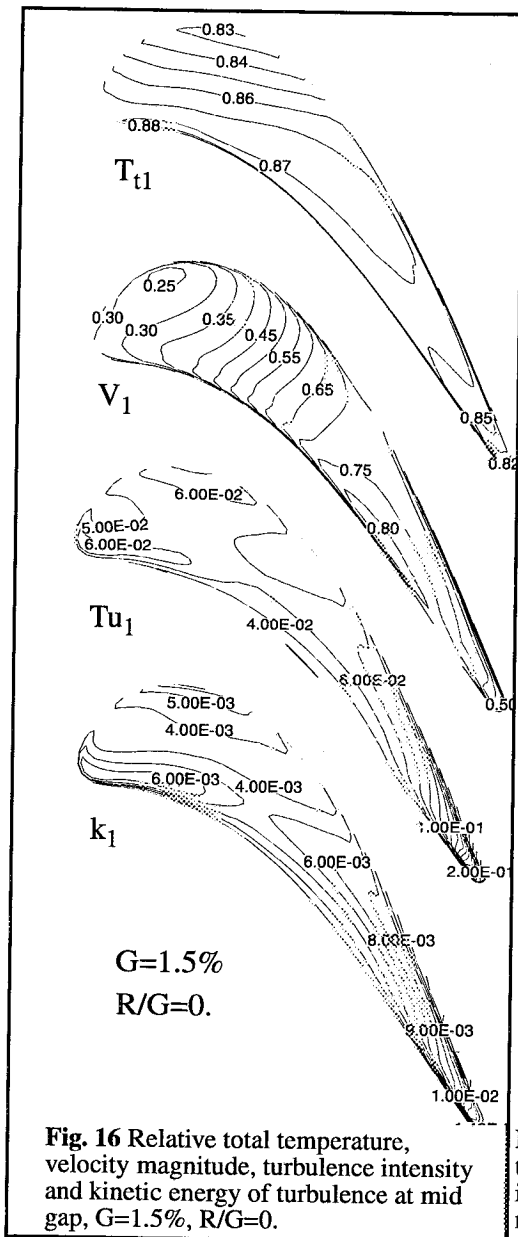


Fig. 15 (a) Contours of $1000 \times \text{Stanton}$ number over the blade tip and (b) line plots of average tip heat transfer. $d=25\%$, $G=3.0\%$

of recess depths is chosen namely, R/G 's of 0, $1/3$, $2/3$ and 1, the latter being even with the blade tip. The reduction of the tip heat transfer is again apparent from that figure, however in this case it appears to be confined mainly to the forward portion. The reason is that for this large clearance gap the gas flows relatively unimpeded over the aft portion of the tip and is less affected by the presence of a casing recess upstream of the blade.

Figure 16 shows plots of relative total temperature, relative velocity magnitude, turbulence intensity and kinetic energy of turbulence for the 1.5% clearance and no upstream recess (base

case). Figures 17 and 18 show the ratios of the same quantities for $G=1.5\%$, $R/G=1$ and $G=3\%$, $R/G=0$ cases to the corresponding quantities of the base case. The purpose of those figures is to aid in determining the cause of change in tip heat transfer by the presence of a recess or by an increase in tip clearance. Referring to Figs. 16, 17 and 18, judging by the levels of turbulence intensity it is likely that the tip flows are all fully turbulent. The drop in heat transfer for the case in Fig. 17 (corresponding to Fig. 14, $R/G=1$) appears to be due to the reduction in the total temperature as well as the flow velocity. In



fact if one assumes a relationship of wall heat flux proportional to velocity ratio to a 0.8 power which is commonly done for a turbulent boundary layer flow, it appears as though most of the drop in heat transfer on the tip can be accounted for by the velocity drop. The same can be said for the 3% clearance where the increase in the tip heat transfer in the attached flow regions is associated with an increase in velocity.

Casing Heat Transfer. Information on the casing heat transfer can be used for cooling of the casing to alleviate "hot spots" or for the purposes of active control of tip clearance. Since the grid rotates at the blade rotation rate, there is no unsteady effect due to rotation which is not accounted for in the calculations.

Figure 19 shows the effect of tip gap height on the circumferentially averaged casing heat transfer. The casing heat transfer as should be expected (Epstein et al, 1985) drops by a large factor (~5) along the axial direction. It is also shown that

the casing heat transfer is markedly affected by the tip clearance gap. The trend is shown to be an increase in heat transfer as the gap widens. The change in the level of heat transfer on the casing is initiated near the blade leading edge and persists past the trailing edge of the blade.

Casing heat transfer is also expected to be influenced by the presence of the recess on the casing. Figure 20 shows the effect of casing recess on the casing heat transfer. The dip on the heat transfer curve corresponds to a location just downstream of the recess where the casing is in the recirculating flow region. There is some reduction on the rate of heat transfer on the casing due to the presence of the recess however it appears to be slight.

Tip Mass Flow

Figure 21(a) is a plot of mass flow rate through the tip clearance normalized by inlet mass flow rate. There is a linear relationship between the mass flow through the clearance and

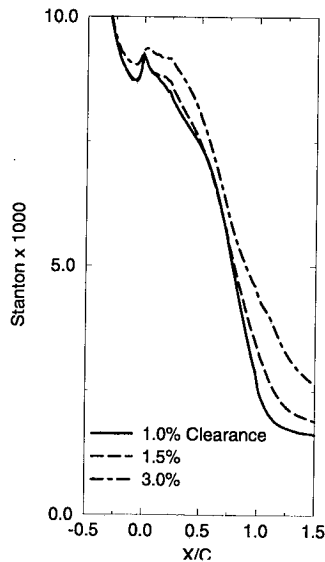


Fig. 19 Circumferentially averaged heat transfer on the casing as affected by the tip clearance height

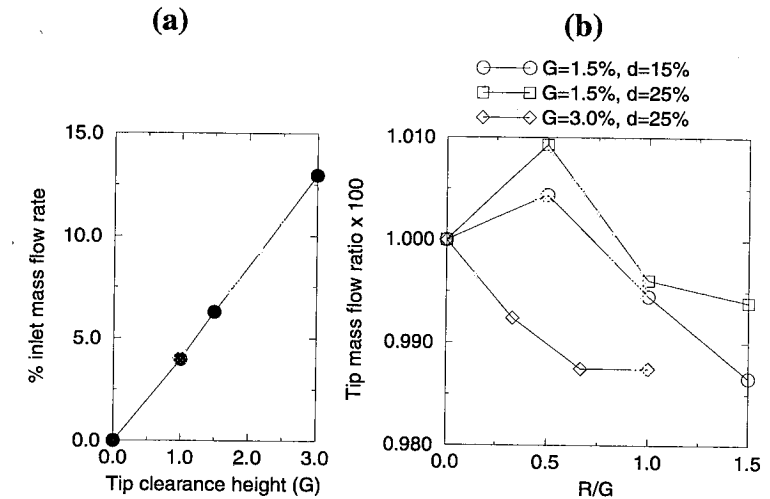


Fig. 21 (a) Tip clearance mass flow rate normalized by the inlet mass flow rate vs. tip clearance height. (b) Tip clearance mass flow rate normalized by the tip mass flow rate without recess vs. recess depth

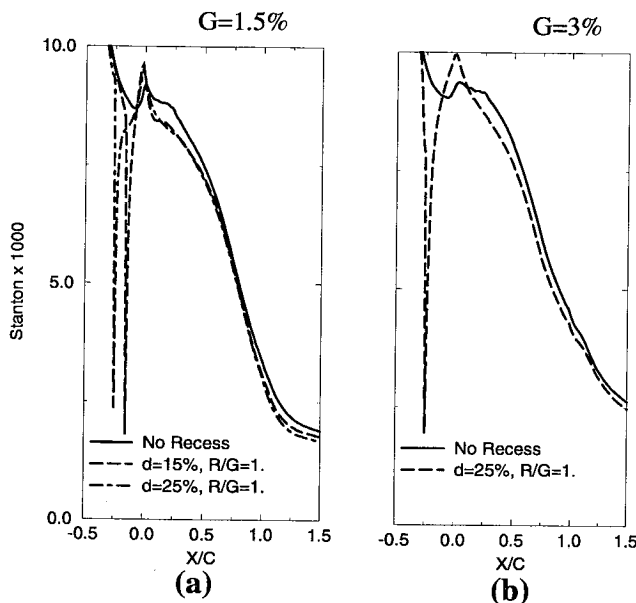


Fig. 20 Casing heat transfer as affected by the presence of the recess. (a) 1.5% and (b) 3% clearance

the tip clearance height. Figure 21(b) shows the mass flow rate through the tip gap as the upstream recess is introduced. The case of 1.5% tip clearance shows an increase in the mass flow rate as recess is introduced initially but shows a reduction thereafter. The mass flow rate is normalized by the tip mass flow rate without the casing recess which is quite small for the $G=1.5\%$ case and therefore the variations in the mass flow due to the presence of the casing recess are quite small. For the 3% clearance the effect of clearance height is more uniform. The reduction in velocity in the tip region of Fig. 17 is due to blockage of the flow coming from the inlet. The fact that the mass flow rate does not change greatly suggests that the flow

through the tip clearance is mainly due to the pressure difference across the blade.

Exit Angle

An important variable in the design of turbine stages is the exit angle. It is known that as the gap widens the unguided flow through the clearance increases and therefore it causes the flow to enter the next set of blades at an angle other than the intended design angle. Figure 22 shows the pitchwise averaged exit angles at two axial locations for the clearance heights considered with and without casing recess. All the runs having the same tip clearance height are represented with the same symbol for the purposes of easy identification. The intended design values at hub, mean and tip are taken from (Timko, 1982) and are also included.

The exit angle associated with zero clearance is represented by a thick solid line without symbols. The no clearance case is overturned near the casing (as near the hub) due to secondary flows. On the other hand, cases with tip clearance have various degrees of underturning proportional to the tip clearance height due to the suction side tip vortex. In Fig. 22(a), the no clearance case has formed a maximum turning limit for all the other cases considered. Addition of a recess has a worsening effect for the case of large tip clearance but has an obvious moderating effect for the lower tip clearance height.

Efficiency

In a previous paper Ameri et al. (1997) presented a method to compute the adiabatic efficiency as a by-product of the heat transfer calculations. The expression used for the calculation of the adiabatic efficiency is:

$$\eta = \frac{T'_{in} - T'_{ex}}{T'_{in} \left[1 - \left(\frac{P'_{ex}}{P'_{in}} \right)^{(\gamma-1)/\gamma} \right]} \quad (2)$$

In the above formula T' and P' signify the mass averaged, absolute total temperature and pressure. The subscripts *in* and *ex*

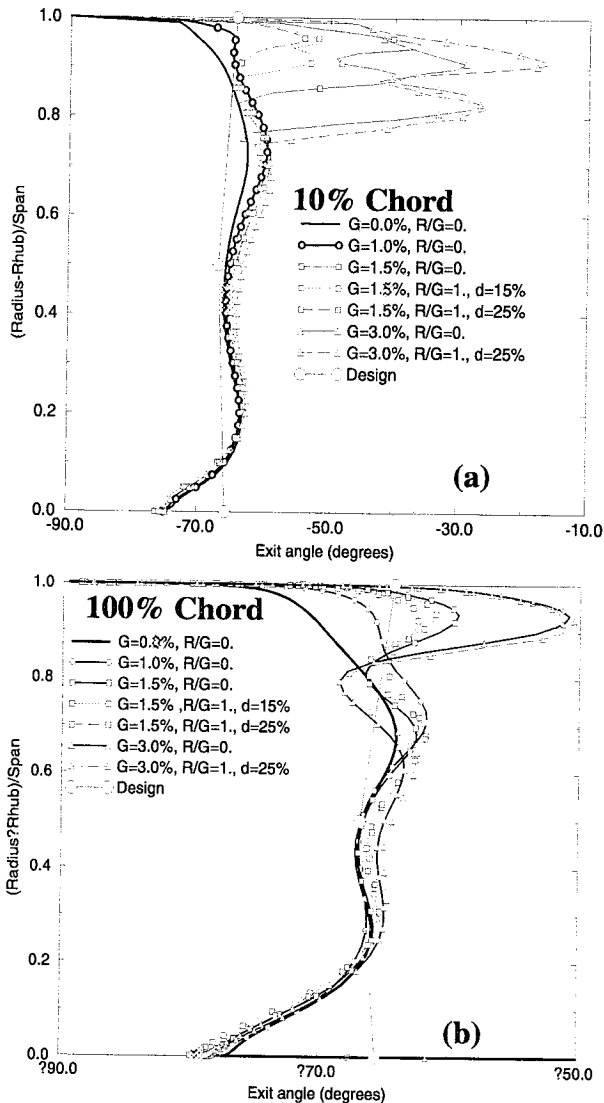


Fig. 22 Exit angle at (a) 10% chord and (b) 100% chord downstream of the blade row

signify the integration locations inlet and outlet of the computational domain and γ is the specific heat ratio. Since the calculations are done with a wall boundary condition other than adiabatic, the exit total temperature is corrected for the heat transfer. Further details can be found in Ameri et al (1997).

For the present set of calculations, the integration planes are located at 50% chord upstream of the blade and 100% chord downstream of the blade. The exit location was selected relatively far downstream to allow for mixing to take place and therefore allow for the differences in efficiency to become apparent. Figure 23 shows the effect of the height of the tip clearance gap on the adiabatic efficiency without the presence of the casing recess. The calculations were performed for the case of no tip clearance as well as 1, 1.5 and 3% tip clearance cases. The solid line is a best fit to the calculations. The variation of efficiency with gap height is seen to be linear with a slope of ~ 1.5 point per percent gap clearance. Both the linearity and the magnitude of the slope agree with the general rule of thumb exercised by designers. The open symbols are calculated from a

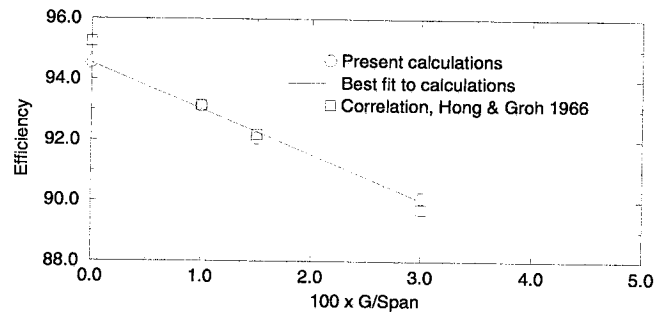


Fig. 23 Adiabatic efficiency as affected by the tip clearance height

graphic correlation put forth by Hong and Groh (1966) as reproduced in NASA SP-290 edited by Glassman(1994). The graphical correlation expresses the efficiency as a fraction of efficiency with no clearance. The no clearance value is obtained by extrapolation. The variation of efficiency as shown in Fig. 23 provides confidence in the results of the calculations. The efficiencies calculated suggest that the losses associated with the tip clearance are approximately 20, 30 and 45 percent of the total losses for the case of 1%, 1.5% and 3% clearance, respectively. This is in agreement with the work of Boyle et al. (1985) and confirms the suggestion made elsewhere that measures taken to reduce the losses due to tip leakage can have a significant effect on the total losses especially when operating with relatively wide tip clearance.

The magnitudes of efficiency calculated here were changed slightly by the presence of the recessed casing. Table 3 shows the calculated efficiency for the 1.5% tip clearance cases considered. For the 1.5% clearance gap the magnitude of the efficiency without the recess was calculated to be 92.06%. For $d=15\%$ at $R/G=0.5$ the magnitude of the efficiency rose to 92.24% which although is a 0.2% increase, it constitutes 8% of the losses due to tip clearance. For the $d=25\%$ the efficiency rose to 92.29% or 9.5% of the tip clearance losses at $R/G=1$. For the $d=15\%$ case the value of efficiency for $R/G=1$ appears to be anomalous although no reason for this drop in efficiency was found. More points might be required to capture the highs and lows of this relationship.

Table 4 contains the efficiency values for the 3% tip clearance cases. The efficiency reaches a maximum of 90.28% or an increase of 0.2% compared to the no recess condition. This is an increase equivalent to recovering 4.5% of the losses due to the tip clearance. A trend can be inferred from the table where there is an intermediate value of casing recess height for which the efficiency reaches a peak. Further increase in the recess height leads to losses in the flow that can offset the gains otherwise attained.

SUMMARY AND CONCLUSIONS

In this paper, results are presented from three-dimensional simulations of flow and heat transfer in an unshrouded turbine rotor passage with and without casing recess. Casing recess is a configuration often found in turbine blade passages. For the purposes of the calculations a generic modern gas turbine blade namely that of first stage rotor of GE-E³ turbine was selected. A multi-block grid was generated to discretize the flow field. Clearance heights of 0%, 1%, 1.5% and 3% of the passage height

TABLE 3. Efficiency, G=1.5%

| | R/G=0 | R/G=0.5 | R/G=1. | R/G=1.5 |
|-------|-------|---------|--------|---------|
| d=15% | 92.06 | 92.24 | 91.85 | 92.16 |
| d=25% | 92.06 | 92.07 | 92.29 | 92.04 |

TABLE 4. Efficiency, G=3%

| | R/G=0 | R/G=1/3 | R/G=2/3 | R/G=1. |
|-------|-------|---------|---------|--------|
| d=25% | 90.09 | 90.28 | 90.15 | 90.03 |

were considered. For the two largest clearance heights considered, different recess depths were studied.

There was an increase in the thermal load on all the heat transfer surfaces considered due to enlargement of the clearance gap.

Introduction of recessed casing resulted in a drop in the rate of heat transfer on the pressure side but the picture on the suction side was found to be more complex for the smaller tip clearance height considered. For the larger tip clearance height the effect of casing recess was a reduction in the suction side heat transfer.

There was a marked reduction of heat load and peak values on the blade tip upon introduction of casing recess, however only a small reduction was observed on the casing itself.

It was reconfirmed that there is a linear relationship between the efficiency and the tip gap height. It was also observed that the casing recess has a small effect on the efficiency.

It was also observed that the recessed casing can have a moderating effect on the flow underturning at smaller tip clearances.

ACKNOWLEDGEMENT

This work was sponsored by the Smart Green Engine Project managed at NASA Lewis Research Center by Mr. Kestutis Civinskis. The authors wish to express their gratitude to Dr. Raymond Gaugler, chief of the Turbine Branch, Mr. Ned Hannum chief of the Turbomachinery and Propulsion Systems Division as well as to Dr. Louis Povinelli chief scientist of the Turbomachinery and Propulsion Systems Division of NASA Lewis Research Center and Director of ICOMP for their support and encouragement of this work. As always we had the benefit of helpful suggestions offered by Mr. Robert Boyle of NASA Lewis Research Center. Some of the computations were performed on the CRAY-C90 of NAS at NASA Ames Research Center.

REFERENCES

Ameri, Ali A., and Steinhorrson, E., 1995, "Prediction of Unshrouded Rotor Blade Tip Heat Transfer," ASME 95-GT-142.
 Ameri, Ali A., and Steinhorrson, E., 1996, "Analysis of Gas Turbine Rotor Blade Tip and Shroud Heat Transfer," IGTI 96-GT-189.
 Ameri, Ali A., and Steinhorrson, E., Rigby, David L., 1997, "Effect of Squealer Tip on Rotor Heat Transfer and Efficiency," ASME 97-GT-128. To be published in the journal of Turbomachinery.
 Boyle, Robert J., Haas, Jeffrey E. and Katsanis, Theodore, 1985, "Comparison Between Measured Turbine Stage Performance

and the Predicted Performance Using Quasi-3D Flow and Boundary Layer Analyses," *J. of Propulsion and Power*, Vol.1 no.3, pp 242-251.

Briley, W. R., Roscoe, D. V., Gilbeling, H. J., Buggeln, R. C. and Sabnis, J. S., 1991, "Computation of Flow Past a Turbine Blade With and Without Tip Clearance," IGTI paper 91-GT-56.

Epstein, A. H., Guenette, G. R., Norton, R. J. G. and Cao Yuzhang, 1985, "Time Resolved Measurements of a Turbine Rotor Stationary Tip Casing Pressure and Heat Transfer Field," AIAA paper 85-1220.

Garg, Vijay, K. and Rigby, David L., "Heat Transfer on a Film-Cooled Blade-Effect of Hole Physics", accepted for presentation at the International Gas Turbine Institute Conference and Exposition, June, 1998, Stockholm, Sweden.

Glassman, Arthur, J., *Turbine Design and Application*, NASA SP-290, 1994.

Haas, Jeffrey, F. and Kofsky, Milton, G., 1979, "Effect of Rotor Tip Clearance and Configuration on Overall Performance of a 12.77- Centimeter Tip Diameter Axial-Flow Turbine," NASA, TM 79025.

Halila, E. E. and Lenahan, D. T., and Thomas, T.T., 1982, "Energy Efficient Engine, High Pressure Turbine Test Hardware Detailed Design Report," NASA CR-167955.

Hong, Yong S, and Groh, F. G., "Axial Turbine Loss Analysis and Efficiency Prediction Method," Rep. D4-3220, Boeing Co., Mar. 11, 1966.

Kaiser, I. and Bindon, P. J., 1997, "The Effect of Tip Clearance on the Development of Loss Behind a Rotor and a Subsequent Nozzle," IGTI paper 97-GT-53.

Menter, Florian R., 1993, "Zonal Two-Equation k- ω Turbulence Models for Aerodynamic Flows," AIAA-93-2906.

Metzger, D. E., Bunker, R. S. and Chyu, M. K., 1989, "Cavity Heat Transfer on a Transverse Grooved Wall in a Narrow Channel," *J. of Heat Transfer*, Vol. 111, pp. 73-79.

Rigby David, L., Ameri Ali, A. and Steinhorrson E., 1997a, "Numerical Prediction of Heat Transfer in a Channel with Ribs and Bleed," IGTI paper 97-GT-431.

Rigby, D. L., Steinhorrson, E., Coirier, W. J., 1997b, "Automatic Block Merging Using the Method of Weakest Descent," AIAA Paper 97-0197.

Rigby, D. L., 1996 "Method of Weakest Descent for Automatic Block Merging," 15th Int. Conf. on Num. Methods in Fluid Dynamics, Monterey, CA, June 1996.

Rigby David, L., Ameri Ali, A. and Steinhorrson E., 1996, "Internal Passage Heat Transfer Prediction Using Multiblock Grids and k- ω Turbulence Model," IGTI paper 96-GT-188.

Schlichting, H. *Boundary Layer Theory*. McGraw-Hill, New York, seventh ed. pp. 312-313.

Steinhorrson, E., Liou, M. S., and Povinelli, L.A., 1993, "Development of an Explicit Multiblock/Multigrid Flow Solver for Viscous Flows in Complex Geometries," AIAA-93-2380.

Timko, L.P., 1982, "Energy Efficient Engine High Pressure Turbine Component Test Performance Report," NASA CR-168289.

Wilcox, D. C., 1994a, *Turbulence Modeling for CFD*, DCW industries, Inc. La Canada, CA.

Wilcox, D. C., 1994b, "Simulation of Transition with a Two-Equation Turbulence Model," AIAA Journal, Vol. 32, No.2, pp.247-255.

REPORT DOCUMENTATION PAGEForm Approved
OMB No. 0704-0188

Public reporting burden for this collection of information is estimated to average 1 hour per response, including the time for reviewing instructions, searching existing data sources, gathering and maintaining the data needed, and completing and reviewing the collection of information. Send comments regarding this burden estimate or any other aspect of this collection of information, including suggestions for reducing this burden, to Washington Headquarters Services, Directorate for Information Operations and Reports, 1215 Jefferson Davis Highway, Suite 1204, Arlington, VA 22202-4302, and to the Office of Management and Budget, Paperwork Reduction Project (0704-0188), Washington, DC 20503.

| | | | | |
|---|---|--|---|--|
| 1. AGENCY USE ONLY (Leave blank) | | 2. REPORT DATE August 1998 | 3. REPORT TYPE AND DATES COVERED Contractor Report | |
| 4. TITLE AND SUBTITLE Effects of Tip Clearance and Casing Recess on Heat Transfer and Stage Efficiency in Axial Turbines | | | 5. FUNDING NUMBERS WU-523-26-13-00 NAS3-27571 | |
| 6. AUTHOR(S) A.A. Ameri, E. Steinthorsson, and David L. Rigby | | | | |
| 7. PERFORMING ORGANIZATION NAME(S) AND ADDRESS(ES) Institute for Computational Mechanics in Propulsion 22800 Cedar Point Road Cleveland, Ohio 44142 | | | 8. PERFORMING ORGANIZATION REPORT NUMBER E-11287 | |
| 9. SPONSORING/MONITORING AGENCY NAME(S) AND ADDRESS(ES) National Aeronautics and Space Administration Lewis Research Center Cleveland, Ohio 44135-3191 | | | 10. SPONSORING/MONITORING AGENCY REPORT NUMBER NASA CR-1998-208514 ICOMP-98-04 | |
| 11. SUPPLEMENTARY NOTES Prepared for the Turbo Expo 98 sponsored by the International Gas Turbine Institute of the American Society of Mechanical Engineers, Stockholm, Sweden, June 2-5, 1998. A.A. Ameri, AYT Corporation, Brook Park, Ohio; E. Steinthorsson, Institute for Computational Mechanics in Propulsion, Cleveland, Ohio; and David L. Rigby, NYMA, Inc., 2001 Aerospace Parkway, Brook Park, Ohio. Responsible person, A.A. Ameri, organization code 5820, (216) 433-8346. | | | | |
| 12a. DISTRIBUTION/AVAILABILITY STATEMENT Unclassified - Unlimited Subject Categories: 34 and 07 This publication is available from the NASA Center for AeroSpace Information, (301) 621-0390. | | | 12b. DISTRIBUTION CODE Distribution: Nonstandard | |
| 13. ABSTRACT (Maximum 200 words) Calculations were performed to assess the effect of the tip leakage flow on the rate of heat transfer to blade, blade tip and casing. The effect on exit angle and efficiency was also examined. Passage geometries with and without casing recess were considered. The geometry and the flow conditions of the GE-E ³ first stage turbine, which represents a modern gas turbine blade were used for the analysis. Clearance heights of 0%, 1%, 1.5% and 3% of the passage height were considered. For the two largest clearance heights considered, different recess depths were studied. There was an increase in the thermal load on all the heat transfer surfaces considered due to enlargement of the clearance gap. Introduction of recessed casing resulted in a drop in the rate of heat transfer on the pressure side but the picture on the suction side was found to be more complex for the smaller tip clearance height considered. For the larger tip clearance height the effect of casing recess was an orderly reduction in the suction side heat transfer as the casing recess height was increased. There was a marked reduction of heat load and peak values on the blade tip upon introduction of casing recess, however only a small reduction was observed on the casing itself. It was reconfirmed that there is a linear relationship between the efficiency and the tip gap height. It was also observed that the recess casing has a small effect on the efficiency but can have a moderating effect on the flow underturning at smaller tip clearances. | | | | |
| 14. SUBJECT TERMS Gas turbine; Heat transfer; Efficiency; Casing recess; Tip clearance | | | 15. NUMBER OF PAGES 18 | |
| | | | 16. PRICE CODE A03 | |
| 17. SECURITY CLASSIFICATION OF REPORT Unclassified | 18. SECURITY CLASSIFICATION OF THIS PAGE Unclassified | 19. SECURITY CLASSIFICATION OF ABSTRACT Unclassified | 20. LIMITATION OF ABSTRACT | |